Considering the plug-flow behavior of the gas phase in nitrifying BAF models significantly improves the prediction of N2O emissions

Justine Fiat, Ahlem Filali, Yannick Fayolle, Jean Bernier, Vincent Rocher, Mathieu Sperandio, Sylvie Gillot

Considering the plug-flow behavior of the gas phase in nitrifying BAF models significantly improves the prediction of N_2O emissions

Justine Fiat[1], Ahlem Filali[1,*], Yannick Fayolle[1], Jean Bernier[2], Vincent Rocher[2], Mathieu Spérandio[3], Sylvie Gillot[4]

[1] Irstea, UR HBAN, CS 10030, F-92761 Antony Cedex, France

[2] SIAAP, Direction Innovation Environnement, 92700 Colombes

[3] LISBP, Université de Toulouse, CNRS, INRA, INSA, Toulouse, France

[4] Irstea, UR REVERSAAL, F-69626 Villeurbanne Cedex, France

* Corresponding author (*ahlem.filali@irstea.fr*)

Abstract

Nitrifying biologically active filters (BAFs) have been found to be high emitters of nitrous oxide (N_2O), a powerful greenhouse gas contributing to ozone layer depletion. While recent models have greatly improved our understanding of the triggers of N_2O emissions from suspended-growth processes, less is known about N_2O emissions from full-scale biofilm processes.

Tertiary nitrifying BAFs have been modeled at some occasions but considering strong simplifications on the description of gas-liquid exchanges which are not appropriate for N_2O prediction. In this work, a tertiary nitrifying BAF model including the main N_2O biological pathways was developed and confronted to full-scale data from Seine Aval, the

largest wastewater resource recovery facility in Europe. A mass balance on the gaseous compounds was included in order to correctly describe the N_2O gas-liquid partition, thus N_2O emissions. Preliminary modifications of the model structure were made to include the gas phase as a compartment of the model, which significantly affected the prediction of nitrification. In particular, considering gas hold-up influenced the prediction of the hydraulic retention time, thus nitrification performances: a 3.5% gas fraction reduced ammonium removal by 13%, as the liquid volume, small in such systems, is highly sensitive to the gas presence. Finally, the value of the volumetric oxygen transfer coefficient was adjusted to successfully predict both nitrification and N_2O emissions.

Keywords: Biofilm, Full-scale, Gas-liquid transfer, Modelling, Nitrification, N_2O

Abbreviations

Symbol	Signification
A, B	Empirical constants of the k_La_{O2} to U_G's power law
a_a	Media specific area (m^2/m^3 of empty reactor)
α, β, F, F_R	Transfer reduction factors (wastewater, salinity, diffusers fouling, overflow)
C_G	Concentration in the gas phase (g/m^3)
C_L	Concentration in the liquid phase (g/m^3)
C_L^*	Saturation concentration in the liquid phase in equilibrium with the gas (g/m^3)
CSTR	Completely stirred tank reactor
D	Diffusivity constant in liquid phase (m^2/d)
DO	Dissolved oxygen (gO_2/m^3)
ε_B	Biofilm fraction (-)
ε_G	Gas fraction (-)
ε_L	Liquid fraction (-)
ε_M	Media fraction (-)
$F_{G\rightarrow L}$	Flux transferred from the gas to the liquid phase (g/d)
F_{N2O}	N_2O production rate (gN/d)
$F_{N2O,G}$	N_2O emission rate (gN/d)
$F_{NH4\ removed}$	Ammonium removal rate (gN/d)
g	Gravitational constant (m/s^2)
K_H	Henry's law constant ($g/m^3/atm$)
k_La	Liquid side volumetric transfer coefficient (d^{-1})
N_2O	Nitrous oxide
N_2O-EF	Nitrous oxide emission factor (% of N-NH_4^+ removed)
N_2O-PF	Nitrous oxide production factor (% of N-NH_4^+ removed)
NH_2OH	Hydroxylamine
NH_4^+	Ammonium
NO	Nitric oxide
NO_2^-	Nitrite
NO_3^-	Nitrate
P_{total}	Pressure (atm)
Q_G	Aeration flow (Nm^3/d)
ρ_B	Dry biofilm density (g/m^3)
ρ_G	Gas density at working temperature (g/m^3)
ρ_L	Water density at working temperature (g/m^3)
ρ_M	Media density at working temperature (g/m^3)
T	Working water temperature (K)
θ	Temperature correction factor (-)
U_G	Superficial gas velocity ($Nm^3/m^2/d$)
V_B	Biofilm volume (m^3)
V_G	Gas volume (m^3)
V_L	Liquid volume (m^3)
V_R	Total volume (m^3)
V_M	Media volume (m^3)
y	Gas molar fraction (mol/mol)
Z	Biofilm thickness (m)

1. Introduction

Biological active filters (BAFs) are submerged fixed-bed biofilm reactors combining solids removal by filtration with the biological conversion of carbon, ammonium and/or nitrate. Since the early eighties, they have been successfully used to treat a variety of urban and industrial wastewaters. Owing to their compactness, flexibility and reliability, BAFs have been widely developed in Europe, especially in large urbanized areas where available space is scarce (Mendoza-Espinosa and Stephenson 1999).

Recent monitoring campaigns suggest that nitrifying BAFs are important sources of nitrous oxide (N_2O), a potent greenhouse gas contributing to global warming and ozone depletion. In China, Wang et al. (2016) monitored nitrifying BAFs over a period of 12 months and reported emissions ranging from 0.02 to 1.26 % of influent total nitrogen load. In France, the two monitoring campaigns performed in tertiary nitrifying BAFs of the Seine Aval plant (the largest plant in Europe) reported higher emission factor values: 1.77% of $N\text{-}NH_4^+$ removed in summer and 3.11% in winter (Bollon et al. 2016). Based on the results of the winter campaign, authors estimated that N_2O emissions contributed to almost 80% of the carbon footprint of the biological nitrogen removal stage of the plant (Filali et al. 2017).

Modelling may represent a very useful tool in view of a better understanding of N_2O production mechanisms and can serve to comprehend the effect of different operational conditions and define mitigation strategies. To this end, existing activated sludge models (ASM) were extended to include NO and N_2O formation during autotrophic nitrification and heterotrophic denitrification. N_2O is an obligate intermediate of the heterotrophic denitrification, and the end product of two main biological pathways by ammonium oxidizing bacteria (AOB) and archaea (AOA) (Schreiber et al. 2012). In the first pathway

(nitrifier nitrification, or NN pathway), N_2O is generated as a by-product of incomplete oxidation of hydroxylamine (NH_2OH) to nitrite (NO_2^-). In the second pathway (nitrifier denitrification, or ND pathway), N_2O is generated upon the reduction of NO_2^-. Several models have been proposed to describe either one of these pathways, but failed to predict N_2O emissions in contrasted conditions, especially when transient conditions of dissolved oxygen (DO) or NO_2^- occurred (Spérandio et al. 2016). Hence, recent models coupling multiple N_2O pathways were proposed to describe and extrapolate the emissions for a wide broad of operating conditions. A detailed review of these models can be found in the literature (Massara et al. 2017; Ni and Yuan 2015). Among them, the model of Pocquet et al. (2016), which couples the two N_2O biological production pathways by AOBs, has been validated on extensive lab-scale datasets. It was found able to predict N_2O emissions for contrasted DO and NO_2^- conditions, and also the respective contributions of NN and ND pathways to the total production of N_2O (Lang et al. 2016).

On the other hand, few models have been proposed to describe the behavior of nitrifying BAFs (Bernier et al. 2014; Vigne et al. 2010; Hidaka and Tsuno 2004; Behrendt 1999; Viotti et al. 2002). They are mainly one dimensional and differ in the number of mechanisms simulated and in the level of complexity considered in their description. Gas-liquid mass transfer of oxygen is one of the mechanisms that received the least attention, probably because of the difficulty to obtain experimental data and of the lack of standardized measurement methods. Biofilm reactors being mass-transfer limited, a good representation of oxygen gas-liquid mass transfer is usually essential to correctly predict nitrification performances. However, little is known about gas-liquid mass transfer in fixed-bed reactors. Some studies investigated the impact of operating conditions and media properties on oxygen transfer, and mostly at lab or pilot scales, and with a clean media bed (Maldonado et al. 2008; Leung et al. 2006; Pérez et al. 2006; Gillot et al. 2005;

Behrendt 1999; Deront et al. 1998). In some occasions, oxygen supply in BAFs was described in a simplified manner, i.e. assuming a constant non-limiting DO concentration through the filter height (Vigne et al. 2010; Viotti et al. 2002); whereas, in others an aeration model was considered to predict the oxygen supply variation with the airflow rate and the profiles of DO throughout the filter (Bernier et al. 2014; Hidaka and Tsuno 2004). However, several simplifications were made: the gas phase was not considered as a compartment of the reactor, i.e. the gas volume was not included in the calculation of the working volume and the evolution of the gas phase composition was neglected. If this representation of gas-liquid exchanges was found sufficient to describe nitrification performances, it may not be appropriate for NO and N_2O prediction. It has to be noted that few modelling studies considered the gas phase as a compartment when describing nitrification in lab-scale (Poughon et al. 1999) and pilot-scale (Behrendt 1999) fixed-bed reactors. Both studies included oxygen transfer as their final objective was to investigate nitrification but provided little information about this parameter. Moreover, N_2O was not adressed in these studies, and N_2O emissions from full-scale nitrifying BAFs were never modeled so far. The increasing concern about greenhouse gas emissions and the sensivity of plant's carbon footprint to N_2O emissions call for an upgrade of full-plant BAF models to include N_2O production pathways.

To this aim, the model proposed by Bernier et al. (2014), calibrated and validated on long term data from full-scale tertiary nitrifying BAFs of the Seine Aval plant, was extended to describe N_2O emissions monitored on this site. Beforehand, it was necessary to assess the relevance of gas-liquid transfer hypotheses for N_2O prediction. In this paper, different successive options related to gas-liquid transfer hypotheses are considered and implemented for a better description of physical characteristics of BAFs and associated mass transfer: gas-hold up was included to estimate a gas volume, the working volume

was estimated considering the gas volume and a mass balance was added on the gas phase to describe the evolution of the gas phase composition. Their relevance is discussed and the newly developed model is evaluated by comparing modeling results with experimental data. Finally, recommendations of experiments are provided in order to better characterize gas-liquid mass transfer in full-scale BAFs.

2. Material and methods

2.1. Experimental data

Data were collected during a 14-day measuring campaign, in winter 2015, on a Biostyr® unit of the tertiary nitrification stage of the Seine Aval plant (Bollon et al. 2016). The unitary surface was 173 m^2, and the media bed - composed of 4 mm polystyrene beads – was 3.5 m high. Data used for modeling included: online measurements of inlet NH_4^+ and NO_3^-, outlet NH_4^+, NO_3^-, DO, pH, temperature, and outlet dissolved N_2O (measured in the water zone above the media, called the overflow). One-off measures of effluent NO_2^- were also performed. Gas emissions were collected in the middle of the overflow with a floating hood. The main operating conditions of the BAF are displayed in Table 1, with the estimated N_2O production and emission rates. The winter period was preferred to the summer period for the following reasons: (i) the duration of the monitoring was longer; (ii) it is characterized by a higher variability of the loading rate, the temperature and the N_2O gas-liquid partition. More details about the measurement procedure and the results can be found in Bollon et al. (2016). Average values presented in Table 1 are slightly different from the original publication, as influent interruptions occurring during backwashing periods were not considered, in order to avoid

computational issues. During these 30 min backwashing events, the filter was considered to be operated at usual influent flow and concentration conditions, but was characterized by a higher detachment rate of particles. A detailed description of the BAF reactor and model inputs are provided in Appendix A.

2.2. Mathematical model

Preliminary modifications made to the model proposed by Bernier et al. (2014) – referred as the "base" model– were related to: (i) the biokinetic model, and (ii) the gas-liquid transfer representation. The biokinetic model was extended in order to include the main biological N_2O production and consumption pathways related to nitrification and denitrification. A stripping term was added on N_2O and other nitrogen compounds. These preliminary modifications are presented thereafter, followed by the modifications made to assess the model sensitivity to gas-liquid transfer hypotheses.

2.2.1. Biochemical and biofilm model

The proposed model is based on an existing co-current up-flow filter model built on the Simulink toolbox of Matlab (Mathworks) to describe the functioning of tertiary nitrifying Biostyr® filters of the Seine Aval plant (Bernier et al. 2014). The main features of the base model are recalled hereafter. A detailed description is provided in Appendix B.

Hydrodynamics in the BAF are described by a series of seven reactors of equal volume, representing the "active zone" where biological conversions occur. Each reactor is composed of a biologically inactive bulk zone, composed of a gas and a liquid compartment, an inert media volume, and two biofilm layers (Figure 1). It should be noted that the gas compartment was not included in the base model. The biofilm model includes

soluble material diffusion, biofilm growth and particular exchange between biofilm layers as well as attachment and detachment. On top of this zone, an additional CSTR representing the overflow is implemented. Because it has low biomass concentrations in comparison with the underneath zone (only resulting from the detachment, no biofilm layer), it is considered "passive". For simplification, the 1.4 m water zone beneath the media bed was not represented in the model because: (i) the concentration of biomass is low and (ii) oxygen gas/liquid transfer is low considering that the influent entering this zone has a DO concentration of 8 mgO_2/L.

Biokinetic reactions are computed within the two biofilm layers. The model, previously describing nitrification and heterotrophic denitrification as two-step reactions, was extended to include the main N_2O pathways. NO and N_2O were added as intermediates of heterotrophic denitrification, with parameters from the original publication of Hiatt and Grady (2008). The two-pathway model proposed by Pocquet et al. (2016) was included to describe N_2O production by AOBs. Sets of parameters were taken from the second case study of Lang et al. (2016), who worked at NH_4^+ and NO_2^- concentrations close to the ones measured on the Seine Aval plant. Appendix C and D present the Gujer matrix of the extended model and the list of parameters, respectively.

2.2.2. Gas-liquid mass transfer model

2.2.2.1. General description of gas-liquid mass transfer

The base model included a gas-liquid transfer equation for oxygen in each reactor. In this study, it was implemented for all gases considered (i: O_2, N_2O, NO and N_2) according to Eq. [1]. Mass transfer limitations being localized at the liquid side for all gases (all having a low solubility), their volumetric transfer coefficient was estimated from the one of oxygen [Eq.2], in application of the penetration theory (Higbie 1935), as done in other

studies (Lizarralde et al. 2018; Vaneeckhaute et al. 2018). The volumetric oxygen transfer coefficient was defined as a function of the superficial gas velocity and temperature (Maldonado et al. 2008; Pérez et al. 2006; Gillot et al. 2005; Fujie et al. 1992) [Eq.3]. The equilibrium concentration with the gas phase was estimated from the partial pressure of the compound i, calculated itself considering its gas molar fraction, the corresponding Henry's law constant and the total pressure in the reactor [Eq.4].

[Eq.1] $$F_{i,G\rightarrow L,n} = \alpha F V_{L,n} k_L a_i (\beta C^*_{i,L,n} - C_{i,L,n})$$

[Eq.2] $$k_L a_i = k_L a_{O2} \sqrt{\frac{D_i}{D_{O2}}}$$

[Eq.3] $$k_L a_{O2} = A * U_G^B \theta^{T-293.15}$$

[Eq.4] $$C^*_{i,L,n} = K_{H,i} y_{i,n} P_{total,n}$$

Where $F_{G\rightarrow L}$ is the flux transferred from the gas to the liquid phase (g/d), α, F and β parameters that respectively account for the impact of wastewater characteristics, fouling of diffusers, and the effect of wastewater salinity on the saturation concentration, V_L the liquid volume (m^3), $k_L a$ the liquid side volumetric transfer coefficient (d^{-1}), C^*_L and C_L the equilibrium and the liquid concentrations respectively (g/m^3), D the diffusion coefficient in water (m^2/d), θ the Arrhenius coefficient describing temperature effect on $k_L a$, T the working water temperature (K), K_H the Henry's law constant ($g/m^3/atm$), y the molar fraction in the gas phase (mol/mol), and P_{total} the pressure in a given reactor (atm). Indices i and n stand for the compound and the reactor in series, respectively.

The transfer rate in the passive zone was reduced by a factor (F_R) compared to the rate in the active zone. The value of this factor, used in the present model, was calibrated in previous work to 0.032 to adjust the simulated effluent DO concentration with the

measured one. The value lies within ranges proposed by Amiel (2002), which is 0.008 to 0.04 of the total mass of oxygen transferred in the reactor.

2.2.2.2. Implementation of a mass balance on the gas phase (simulations #4 and #5)

The base model assumed the same gas composition over the BAF height with O_2 molar fraction set to 0.21 in all reactors (atmospheric value). In this study, a mass balance on the gas phase was added to describe the evolution of the gas composition [Eq.5]. Its implementation required several modifications of the model: inclusion of a gas volume, first to calculate the actual air/water proportion employed for total pressure estimation (set arbitrarily to 5/95% in the base model), then to estimate the working volume, and modification of k_La_{O2} accordingly (modification of k_La_{O2} calculation to make it consistent with the gas hold-up). Therefore, preliminary simulations were performed (simulations #1 to #3) to assess their impact on nitrification and N_2O predictions; which are described in the next sections. Mass balance was first added on O_2 only to assess its single impact on simulation results (simulation #4), and then it was implemented for all gases (simulation #5).

[Eq.5] $$V_{G,n}\frac{\partial C_{i,G,n}}{\partial t} = \left(Q_{G,n-1}C_{i,G,n-1} - Q_{G,n}C_{i,G,n}\right) - V_{L,n}\alpha F k_L a_i(\beta C^*_{i,L,n} - C_{i,L,n})$$

Where Q_G is the air flow rate (Nm^3/d), C_G the concentration in the gas phase (g/m^3), and V_G the gas volume (m^3).

2.2.2.3. Evolution of the volumetric oxygen transfer rate with the superficial gas velocity (simulation #1)

The base model of Bernier et al. (2014) used k_La_{O2} values and airflow evolution curves taken from the experiments of Gillot et al. (2005), who investigated oxygen transfer in a pilot-scale biofilter operated in similar conditions as those simulated (for more details see Section 4.3). The main difference being that the pilot-scale study was performed in clean water and with unseeded media. The application of the correlation proposed by Gillot et al. (2005) resulted in severe underestimation of nitrification. Consequently, authors increased k_La_{O2} values to meet effluent ammonium concentration.

In this study, we decided to get back to the correlation from Gillot et al. (2005) because it quantified the effect of increased superficial gas velocity both on gas hold-up and oxygen transfer rate evolution (both parameters being considered in our model). A first simulation was performed using these data (#1), and results were compared to the base model predictions (#0).

2.2.2.4. Modification of the pressure calculation considering a variable gas hold-up (simulation #2)

In the base model, pressure inside the BAF was calculated considering the pressure exerted by a 5/95% air/water volume. In this work, the partition between mobile phases was calculated from their actual fractions in the BAF, according to [Eq.6].

For the gas fraction, the relation from Gillot et al. (2005), which positively correlates the gas hold-up to the superficial gas velocity [Eq.7], was chosen, as it was obtained under similar operating conditions. The gas hold-up was considered as homogenous in the BAF for simplification.

The liquid fraction was deduced from the others, the sum of air, liquid, media and biofilm fractions being equal to one [Eq.8]. The biofilm fraction was estimated from the biofilm thickness according to Eq. [9]. The latter is a function of filtration, detachment and biomass growth. Consequently, the biofilm fraction varies with time and along the BAF height. The media fraction is a fixed value, equal to 0.64, which was considered homogeneous in the BAF for simplification.

[Eq.6] $$P_{total,n} = gh_n \left(\frac{\varepsilon_G}{\varepsilon_G + \varepsilon_{L,n}} \rho_G + \frac{\varepsilon_{L,n}}{\varepsilon_G + \varepsilon_{L,n}} \rho_L \right) * (10^{-3}/101325)$$

[Eq.7] $$\varepsilon_G = 2.9\ 10^{-2} - 4.1\ 10^{-4} U_G + 6.8\ 10^{-5} U_G^2$$

[Eq.8] $$\varepsilon_{L,n} = 1 - \varepsilon_G - \varepsilon_M - \varepsilon_{B,n}$$

[Eq.9] $$\varepsilon_{B,n} = Z_n a_a$$

Where g is the gravitational constant (m/s^2), ε_G, ε_L, ε_M, and ε_B the gas, liquid, media and biofilm fractions respectively, ρ_G, ρ_L, ρ_M and ρ_B the associated densities at working temperature (g/m^3), Z the biofilm thickness (m) and a_a the media specific area (m^2/m^3). The multiplication by $10^{-3}/101325$ is used to convert pressure from Pa to atm.

2.2.2.5. Modification of the working volume calculation considering the gas volume (simulation #3)

The liquid volume (i.e. the working volume) is commonly assumed to be the interstitial volume due to the reactor porosity. In BAFs, this working volume is actually occupied by an air/water mixture as both are injected into the system. Consequently, the liquid volume should be calculated considering the gas volume [Eq.10], which is deduced from the gas hold-up [Eq.11].

[Eq.10] $$V_{L,n} = V_{R,n} - V_{M,n} - V_{B,n} - V_{G,n}$$

[Eq.11] $$V_{G,n} = \varepsilon_G V_{R,n}$$

Where V_R, V_M and V_B are the total, media and biofilm volumes (m^3).

2.2.3. Synthesis of the performed simulations

The impact of each hypothesis on the prediction of nitrification performances and N_2O gas-liquid partition was tested in a series of simulations. Modifications were implemented step by step, as described in Table 2. An additional simulation (#6) was performed after calibrating the K_La_{O2} value while keeping biokinetic parameters unchanged. It has to be noted that this paper is not intended to discuss into details the mechanisms of N_2O production in BAFs. It is focused on the evaluation of the impact of gas-liquid mass transfer representation on N_2O gas-liquid partition, thus on predicted off-gas N_2O concentrations.

Each dynamic simulation was preceded by a 100-day pseudo-steady-state using average constant inputs from Table 1 and data describing the influent composition (more details can be found in Appendix A). Only dynamic predictions are presented in the paper. If "average" is indicated, it stands for an average of the dynamic simulation outputs for the period. Model outputs were compared to effluent characteristics measured on the studied BAF over 14 days (Appendix A).

2.3. Calculation of N_2O emissions and factors

The N_2O production rate was calculated considering the sum of the production rate by AOBs and the net production rate by heterotrophs. The N_2O emission rate is calculated as the sum of fluxes stripped in each reactor [Eq.12]. As long as the mass balance on

gaseous N_2O had not been added (simulations #0 to #4), it was the only way to calculate this emission rate. Afterwards, it could also be calculated as the product of the off-gas N_2O concentration and the airflow rate. Both calculations gave the exact same result for a given simulation (verified on simulations #5 and #6). The N_2O emission and production factors are respectively calculated by dividing the emission and production rates by the ammonium removal rate according to Eq. [13] and [14].

[Eq.12] $$F_{N2O,G} = -\sum_{n=1}^{8} F_{N2O,G\rightarrow L,n}$$

[Eq.13] $$N_2O - EF = \frac{F_{N2O,G}}{F_{NH4\ removed}}$$

[Eq.14] $$N_2O - PF = \frac{F_{N2O}}{F_{NH4\ removed}}$$

Where F_{N2O} and $F_{N2O,G}$ are respectively the N_2O production and emission rates (gN/d), $F_{N2O,G\rightarrow L}$ the N_2O flux transferred from the gas to the liquid phase (gN/d), $N_2O - PF$ and $N_2O - EF$ the production and emission factors respectively (% of $N\text{-}NH_4^+$ removed), and $F_{NH4\ removed}$ the ammonium removal rate (gN/d).

3. Results

3.1. Simulation results obtained with the base model (simulation #0)

A simulation run was performed with the base model (simulation #0, Table 2), for which the results are presented in Appendix E.

On average, predicted and observed effluent NH_4^+ and NO_3^- concentrations were 4.9 and 28.0 mgN/L, against 5.7 and 27.7 mgN/L. Nitrite concentration was correctly predicted (0.65 against 0.64 mgN/L measured), as well as effluent DO concentration (7.3 against 7.1 mgO_2/L measured). In addition, the model was also found able to catch the main dynamics of effluent concentrations (DO, ammonium, nitrate and nitrite).

N_2O production was overestimated by 30% (39.1 against 30.0 kgN/d), but most importantly the model was not able to describe the partition of N_2O between the gas and liquid phases. N_2O emission rate was overestimated by 89%, while the dissolved N_2O was underestimated by 88%. All in all, the emitted to produced N_2O ratio was 97%, while the measured one was 65%, questioning the performance of the gas-liquid transfer model. On the other hand, the oxygen transfer prediction was satisfying as nitrification rate was correctly predicted as well as effluent DO concentration.

3.2. Impact of gas-liquid transfer hypotheses implementation

Table 3 presents a summary of model predictions in terms of nitrification performance, N_2O production rate and its gas-liquid partition for each simulation. Results are detailed in the following sections.

3.2.1. Evolution of the volumetric oxygen transfer rate with the superficial gas velocity (simulation #1)

For an average superficial gas velocity of 299 $Nm^3/m^2/d$, the k_La_{O2} was 91 h^{-1} with the initial model. After modifying the k_La_{O2} to U_G's correlation [Eq. 7], it decreased to 65 h^{-1}. Consequently, the mass of O_2 transferred to the liquid phase dropped substantially which negatively impacted nitrification performances (ammonium removal rate passed from 587 to 449 kgN/d).

N_2O production rate decreased in a lower extent (from 39.1 to 34.1 kgN/d), resulting in an increase of predicted N_2O-PF from 6.7 to 7.6%. According to the model, the net N_2O production by AOBs decreased by 11 kgN/d, and its proportion consumed by heterotrophic bacteria remained constant (53%, i.e. 6 kgN/d), resulting in a lower net N_2O production rate. The emitted to produced N_2O ratio decreased from 97 to 93% as k_{LaN2O} decreased with k_{LaO2}, reducing N_2O transfer to the gas phase.

3.2.2. Modification of the pressure calculation considering a variable gas hold-up (simulation #2)

In simulation #2, the gas hold-up was estimated according to Eq. [7]. The gas hold-up was used to calculate the gas saturation, i.e. the proportion of gas in the gas/liquid mixture, and the reactor pressure according to Eq. [6]. A 5% gas saturation was set arbitrarily in simulations #0 and #1.

Depending on the superficial gas velocity, the gas hold-up was 3.5% on average during the 14-day period. This resulted in a mean gas saturation of 13% in the active zone (Figure 2), which was about three times higher than the previously imposed value. The decrease of gas saturation over the filter height was related to the thinner biofilm, which induced higher liquid volume, while gas hold-up was considered as homogeneous in the BAF. In the passive zone, gas saturation was directly equal to gas hold-up, since there was no media. Consequently, gas saturation considered in simulations #0 and #1 was higher in this zone. The modifications did not significantly affect pressure values in the BAF (-1% on average), which resulted in similar nitrification performance (444 and 449 kgN/d after and before modification, respectively) and N_2O production rates (34.0 and 34.1 kgN/d respectively). Likewise emitted to total N_2O ratio was similar (93.0 against 93.1%).

3.2.3. Modification of the working volume calculation considering the gas volume (simulation #3)

The repartition of media, biofilm, liquid and gas volumes in the active zone is presented on Figure 3 (left panel); whereas the evolution of the hydraulic retention time (HRT) is presented on the right panel.

Accounting for the gas volume (21 m^3 on average) reduced the liquid volume from 160 to 140 m^3. The HRT was therefore reduced in the same proportion (13%), which resulted in lower mass of autotrophic biomass stabilized in the BAF and reduced nitrification performances (ammonium removal rate passed from 444 to 390 kgN/d). Total HRT in the BAF was 29.9 and 27.9 min before (#2) and after (#3) including gas hold-up to calculate the remaining liquid volume.

For simplification, gas hold-up was considered homogeneous over space. On the other hand, the biofilm fraction was not homogeneously distributed. In agreement with experimental observations (Azimi et al. 2010; Vigne 2007), the model predicted a decrease of the biofilm thickness over the height that followed the evolution of nitrogen removal. Consequently, the volume available for water, thus NH_4^+ removal, was more affected at the bottom of the reactor (ammonium removal rate -21% and -8% at the bottom and the top of the BAF, respectively).

3.2.4. Implementation of a mass balance on the gas phase (simulations #4 and #5)

Figure 4 displays the evolution of O_2 (left panel), NO and N_2O (right panel) gas molar fractions over the BAF height. Simulation results indicated a depletion of O_2, as it was transferred to the liquid phase: O_2 gas fraction decreased from 0.21 to 0.18 on average. This reduced the concentration gradient at the gas-liquid interface by 8% on average in

the active zone, lowering the O_2 transfer rate. Consequently, ammonium removal rate was reduced from 390 to 359 kgN/d (-8%).

At the contrary, the N_2O gas molar fraction increased over the BAF height as it got stripped from the liquid. On average, its fraction increased from 3 10^{-7} to 1.3 10^{-4} and its concentration in the off-gas was 298 ppm, i.e. almost 10^3 times the atmospheric concentration (~ 328 ppb). This enrichment decreased the gradient concentration at the gas-liquid interface for stripping and the associated total N_2O flux from liquid to gas. The results were similar for NO in a lower extent (5 ppm in the off-gas). Models #1 to #4 highly overestimated the emitted to produced N_2O ratio (over 90% predicted against 65% measured). After integrating the gas enrichment in NO and N_2O, the predicted ratio for simulation #5 (71%) was closer to full-scale data.

The NO and N_2O gas fraction profiles were related to their production within the filter. The latter increased over the reactor height, as NO and N_2O were produced during nitrification. The associated transfer rates from the bulk to the gas phase therefore increased over the BAF height, which explained the accumulation of NO and N_2O in the gas phase. Finally, their small evolutions between 3.5 and 4.25 meters were due to the lower gas-liquid transfer rates in the passive zone.

The same net N_2O production by AOBs was modelled in simulations #4 and #5. However, the available dissolved N_2O to be reduced by heterotrophs was higher in simulation #5, which induced a higher consumption rate, i.e. a lower net N_2O production. Consequently, the net N_2O production rate was 26.3 against 28.0 kgN/d in simulation #4.

3.3 Simultaneous prediction of nitrification performances and N_2O emissions (model calibration, simulation #6)

In order to recover nitrification performances, k_{LaO2} values were increased from 65 to 117 h^{-1} on average, by increasing the A constant of Eq.[3] from 43 to 81 (simulation #6). Figure 5 represents measured and predicted effluent NH_4^+, NO_3^-, DO concentrations, emitted to produced N_2O ratio, as well as airflow rate and effluent temperature.

Predicted and measured average effluent concentrations were very similar: 5.4 vs. 5.7 mgN/L for NH_4^+, 27.6 vs. 27.7 mgN/L for NO_3^-, 6.5 vs. 7.1 mg/L for DO, and 0.71 vs. 0.64 mgN/L for NO_2^- (not shown on Figure 5), respectively. Their dynamics were also well described by the model.

The modification of k_{LaO2} increased k_{LaN2O} [Eq.2], thus increasing the emitted to produced N_2O ratio from 71 to 74%. The N_2O emission factor was however closer to experimental data (4.5% vs. 5.2% before calibration), as the NH_4^+ removal rate was better described (Table 3). The predicted ratio followed the main trends as experimental data. Its value is well predicted from days 0 to 3 and days 8 to 14. The drop from day 3 to day 8 was due to an increase of the airflow rate - related to a peak of ammonium load - and to a decrease of temperature. Measures reported a drop of the emitted to produced N_2O ratio more pronounced than model predictions. The effect of temperature on Henry's constants was included in the model, according to the literature (Sander 2015). The difference of the emitted to produced N_2O ratio between observations and model predictions is due to an overestimation of N_2O production which is much more pronounced at this period (+44%) compared to the rest of the period (+4%). Model results suggested an increase of N_2O production by AOBs, and a decrease of N_2O consumption by heterotrophs, related to high O_2 transfer rates.

After calibrating k_La_{O2} value, and without any calibration of N_2O parameters, simulation results were closer to experimental data than predictions from the initial model. N_2O concentrations were 407 ppm and 0.44 mgN/L in the off-gas and the effluent respectively, against 318 ppm and 0.50 mgN/L measured.

4. Discussion

4.1. Considering gas enrichment is essential to predict N_2O emissions

Whereas the plug flow behavior of the liquid phase is usually considered in BAF models, it has rarely been taken into account for the gas phase (Bernier et al. 2014; Vigne et al. 2010; Hidaka and Tsuno 2004; Viotti et al. 2002), with the exception of some studies performed at small-scale on oxygen gas-liquid mass transfer (Cruvellier et al. 2017; Poughon et al. 1999). To our best knowledge, the BAF model developed in this study is to date the only one describing both oxygen and N_2O gas-liquid mass transfer and moreover at full-scale.

Results of this study highlighted significant differences in model predictions when considering a constant (well-mixed hypothesis) or a variable gas composition. With a constant gas composition corresponding to that of ambient air (simulation #0), the model was able to predict nitrification performances but failed to describe the emitted to produced N_2O ratio as it overestimated N_2O stripping (see Table 3). It was only when a mass balance on the gas phase was included, that the model correctly described the emitted to produced N_2O ratio. Gas enrichment along the BAF height (from bottom to top:

300 ppb to 298 ppm, in simulation #5) highly decreased the driven potential of N_2O transfer [Eq.1], allowing a larger fraction of N_2O to remain soluble.

The inclusion of this mass balance impacted much more NO and N_2O than O_2 transfer (simulation #4). It induced gas depletion in O_2 by 8% only, lowering nitrification performances to a small extend (-8% between simulations #3 and #4). Even when k_La_{O2} and k_La_{N2O} were increased by the same proportion in simulation #6, the impact was more pronounced for N_2O outflow molar fraction (+36%) compared to the one of O_2 (-7%). This result is explained by the fact that oxygen is respectively 2 and 19 times less soluble than NO and N_2O ($K_{H,O2}$ = 1.5 10^{-5} ; $K_{H,NO}$ = 2.3 10^{-5} ; $K_{H,N2O}$ = 2.8 10^{-4} mol/m^3/atm at 15°C) and its content in the ambient air is much higher.

In sum, modelling the gas-phase as a plug-flow reactor, similarly to the liquid phase, appears to be essential to model gas-liquid N_2O exchanges. Otherwise, predicted N_2O off-gas concentration would be highly underestimated and N_2O stripping overestimated. If dissolved N_2O concentration is not measured (which is often the case), this could lead to unnecessary calibration of the biokinetic model parameters to fit measured off-gas N_2O concentration. This result is in accordance with other studies dealing with gases of higher solubility than O_2 like CO_2 (Sperandio and Paul 1997). This recommendation stands not only for BAFs but also for any process having a plug-flow behavior of the gas phase, such as activated sludge processes with bubble aeration.

4.2. Considering gas hold-up largely impacted nitrification prediction

Modifications have been made to the initial BAF model to take into account the minimum physical phenomena that allow a proper description of N_2O emissions. These

affected predictions of nitrification performances, in particular the consideration of the gas phase as a compartment of the model.

The gas phase was added as a compartment of the BAF by including gas hold-up according to Eq. [8], which was 3.5% of the active volume on average. Results indicated that it highly decreased nitrification performances when considered to calculate the working volume (-13%). This result may seem surprising given the small gas fraction. However, it should be reminded that the BAF system is mostly filled with polystyrene materials (64% of the reactor volume in the active zone). Unlike suspended growth systems, such as conventional activated sludge, the working volume in BAFs cannot be considered to be the reactor volume. The volume available for water is relatively small (about 26% of the active zone, considering that 10% is occupied by the biofilm on average), making the liquid fraction very sensitive to gas variations. Such feature could help improving the prediction of nitrogen removal in case of hydraulic peak-loads or episodes of high aeration rates, both operational parameters reported as requiring additional calibration of the BAF model parameters (Vigne et al. 2010).

The sum of all modifications resulted in a large underestimation of ammonium removal rate (-39%), which required a calibration. Given the capacity of the initial model to describe nitrification with biokinetic parameters from the literature (simulation #0), it seemed more adapted to calibrate transfer model parameters only.

4.3. Calibration procedure and recommendations

The extended model was calibrated after modification of the gas-liquid transfer coefficient to recover average nitrification performances. Similarly to Bernier et al. (2014), our approach was to increase k_La_{O2}, considering that gas-liquid exchanges should be higher in a functioning BAF compared to a clean media bed (unseeded and working

with clean water), which has been observed in previous studies (Reiber and Stensel 1985; Stenstrom et al. 2008). We did not, however, modify the correlation between gas hold-up and superficial gas velocity [Eq.6]. The main elements supporting these assumptions are the differences in terms of fixed-bed properties and hydraulics. This is discussed hereinafter with our current understanding of the physical mechanisms involved in such systems, and supported by simulation results and a literature review.

4.3.1. Slight evolution of global gas hold-up

A functioning BAF differs from a clean media bed by the effluent composition which could affect the surface tension (Gunde et al. 1992; Sridhar and Rami Reddy 1984); but also by lower bed porosity due to the development of the biofilm on the media (increasing particle size) and within the media bed interstices. Likewise, based on a set point value of the headloss, BAFs are regularly backwashed to avoid too much biofilm and particles accumulation (Bernier et al. 2016).

In a pilot BAF study, Stenstrom et al. (2008) attributed the higher oxygen transfer efficiency observed in process water to an increase of gas hold-up. This assumption was based on a naked eye observation through an observation port on the column, which revealed that gas bubbles were retained by the media for a few seconds before being washed away. Previous work on lab-scale fixed-beds –operated in co-current upflow mode and in clean conditions– has shown that gas hold-up was negatively correlated with packing size (Collins et al. 2017; Maldonado et al. 2008; Kies et al. 2005) and negatively with bed porosity (Collins et al. 2017; Maldonado et al. 2008). According to Collins et al. (2017), and Maldonado et al. (2008), the increase of gas hold-up is mainly due to a higher static gas fraction (also called stagnant gas hold-up); which is attributed to increased gas to particles contact area and higher surface tension forces.

However, it is likely that the increase of the static gas fraction is less pronounced in a functioning backed bed system compared to a clean water system due to the lower liquid surface tension and associated capillarity forces. This latter is expected to favor the deformation of bubbles and their breakup. Considering that bubbles size was found to be calibrated by the pores size (Chen et al. 2017; Bordas et al. 2006), a distribution with lower bubble sizes is to be found in a functioning BAF. Thanks to their reduced size, bubbles should have the ability to evolve more easily within the bed (Deshpande et al. 2018), thus reducing the static gas fraction and compensating the increase of the dynamic gas hold-up.

To evaluate the hypothesis based on a slight evolution of global gas hold-up, an additional simulation was performed (results not shown) by increasing gas hold-up along with k_La_{O2}. This led to a severe reduction of ammonium removal rate, as the HRT highly decreased (see Section 4.2). In order to achieve correct ammonium removal (81%), k_La_{O2} had to be increased to 162 h^{-1}, which corresponded to an average gas hold-up of 8.6%. These high values –far beyond literature ranges in clean systems– increased the emitted to produced N_2O ratio from 74 to 75%, moving it further away from experimental data (65%).

This result supports the hypothesis of a less pronounced evolution of global gas hold-up in a functioning BAF compared to a clean media bed. However, experimental validation is necessary. It would require characterizing the evolution of the different gas fractions (static and dynamic) and bubbles size with water composition (such as surface tension) and backed bed properties (such as bed porosity). Application of new characterization methods such as tomography could be very useful (Collins et al. 2017; Chen et al. 2017).

4.3.2. Evolution of oxygen transfer coefficient

The main elements supporting a higher gas/liquid transfer rate in a functioning BAF compared to a clean media bed are:

- As mentioned above, a slight evolution of gas hold-up coupled with a reduction of the distribution of bubbles size would increase the interfacial area ;
- The decrease of the bed porosity due to the biofilm coupled with a slight evolution of gas hold up would increase the gas to liquid volume ratio. According to the present model, the biofilm fills about 9% of the active zone. This would theoretically increase the gas to liquid volume ratio from 0.097 to 0.130 ;
- The reduced liquid volume would induce a higher local liquid velocity in the bed, therefore increasing the slip velocity between liquid and bubbles and consequently the liquid side mass transfer coefficient k_L (Maldonado et al. 2008) ;
- Lower bed porosity is expected to influence bubbles movement in the void fraction inducing increased turbulence in the bubble wake and consequently increased k_L (Kherbeche et al. 2013).

In summary, the mechanisms affecting mass transfer parameters in full-scale BAFs are not fully understood, especially the combined effect of bed porosity and particle size changes in the gas hold-up and oxygen transfer needs to be evaluated. In this study, k_La_{O2} and gas hold-up were both found to highly impact nitrification performances and gas to liquid partition of N_2O. It was chosen to partially decorrelate those parameters as we kept the gas hold-up corresponding to that of a clean media bed (Gillot et al. 2005) while increasing the value of k_La_{O2}. This way, it was possible to correctly predict both the mass transfer of oxygen (with nitrification performances and effluent DO concentration being well predicted) and N_2O (as its gas to liquid partition was well predicted). However, experiments are necessary to validate these hypotheses. Gas-liquid transfer

measurements with a clean media bed against a colonized one at different colonization degrees (i.e. progressive reduction of the bed porosity), would provide useful information for model calibration. The experimental design should also evaluate the evolution of bubble's size and shape for dissociating the impact of the presence of the biofilm on the liquid side mass transfer coefficient (k_L) and on the interfacial area (a). Furthermore, experiments should also be performed in full-scale BAFs to assess the gas distribution within the media bed and global k_La_{O2} for various superficial gas velocities.

5. Conclusion

In this work, a tertiary nitrifying BAF model, previously validated on long-term data of the Seine Aval plant, was extended to include the main biological production and consumption pathways of N_2O. Hypotheses related to gas-liquid exchanges were successively implemented in the model, in order to assess their relevance to describe nitrification and N_2O emissions. Model predictions were confronted to experimental data from a 14-day measuring campaign on Seine Aval. The main conclusions are:

- Without considering the mass balance on the gas phase, the model was able to successfully describe nitrification and the order of magnitude of N_2O production rate. It was, however, unable to predict the N_2O gas-liquid partition, highly overestimating the emitted to produced N_2O ratio (over 90%, against 65%);
- Including the mass balance for the gas phase, allowed the model to describe N_2O emissions, predicting gas enrichment over the BAF height (300 ppb to 298 ppm);
- Preliminary modifications of the model heavily impacted the prediction of nitrifying performances. In particular, the inclusion of a gas compartment decreased the liquid volume, i.e. the HRT, and consequently ammonium removal by 13%;

- In the absence of experimental data on gas-liquid transfer in full-scale BAFs, the model was calibrated by increasing k_La_{O2} from 65 to 117 h^{-1};
- The calibrated model successfully described nitrification and N_2O production and emissions.

  In future work, the extended model will be confronted to a second dataset and evaluated on its ability to predict nitrification and N_2O emissions for contrasted operating conditions. After validation, it will be used to get a further insight into the mechanisms leading to high N_2O emissions in full-scale nitrifying BAFs.

Acknowledgments

This PhD work is part of the "N_2Otrack" project ANR-15-CE04-0014-02 funded by the French National Research Agency. Authors would also like to thank the research program Mocopée http://www.mocopee.com/.

References

Amiel, C. 2002. Mise au point d'une méthodologie de détermination du transfert d'oxygène application aux biofiltres. PhD thesis, Institut National des Sciences Appliquées, Toulouse, France.

Azimi, S., P. Ferreira, V. Rocher, c. Paffoni, and A. Goncalves. 2010. Vieillissement des unités de biofiltration des eaux usées : bilan après 10 années de fonctionnement. *L'eau, l'Industrie, les Nuisances* 339:58-66.

Behrendt, J. 1999. Modeling of aerated upflow fixed bed reactors for nitrification. *Water Science and Technology* 39 (4):85-92.

Bernier, J., V. Rocher, S. Guerin, and P. Lessard. 2014. Modelling the nitrification in a full-scale tertiary biological aerated filter unit. *Bioprocess and Biosystems Engineering* 37 (2):289-300.

Bernier, J., V. Rocher, and P. Lessard. 2016. Initial and hourly headloss modelling on a tertiary nitrifying wastewater biofiltration plant. *Environmental Technology* 37 (10):1188-1196.

Bollon, J., A. Filali, Y. Fayolle, S. Guerin, V. Rocher, and S. Gillot. 2016. N2O emissions from full-scale nitrifying biofilters. *Water Research* 102:41-51.

Bordas, M.-L., A. Cartellier, P. Séchet, and C. Boyer. 2006. Bubbly flow through fixed beds: micro-scale experiments in the dilute regime and modelling. *AICHE J* 52 (11):3722-3743.

Chen, Z., J. Yang, D. Ling, P. Liu, I. M. S. K. Ilankoon, Z. Huang, and Z. Cheng. 2017. Packing Size Effect on the Mean Bubble Diameter in a Fixed Bed under Gas–Liquid Concurrent Upflow. *Industrial & Engineering Chemistry Research* 56 (45):13490-13496.

Collins, J. H. P., A. J. Sederman, L. F. Gladden, M. Afeworki, J. D. Kushnerick, and H. Thomann. 2017. Characterising gas behaviour during gas-liquid co-current up-flow in packed beds using magnetic resonance imaging. *Chemical Engineering Science* 157:2-14.

Cruvellier, N., L. Poughon, C. Creuly, C. G. Dussap, and C. Lasseur. 2017. High ammonium loading and nitrification modelling in a fixed-bed bioreactor. *Journal of Water Process Engineering* 20:90-96.

Deront, M., F. M. Samb, N. Adler, and P. Péringer. 1998. Volumetric oxygen mass transfer coefficient in an upflow cocurrent packed-bed bioreactor. *Chemical Engineering Science* 53 (7):1321-1330.

Deshpande, S. S., J. Walker, J. Pressler, and D. Hickman. 2018. Effect of packing size on packed bubble column hydrodynamics. *Chemical Engineering Science* 186:199-208.

Filali, A., J. Bollon, Y. Fayolle, S. Guerin, V. Rocher, and S. Gillot. 2017. Nitrous oxide emissions from full-scale nitrifying and denitrifying BAF reactors. Paper read at 10th Internation Conference on Biofilm Reactors, at Dublin.

Fujie, K., H.-Y. Hu, Y. Ikeda, and K. Urano. 1992. Gas-liquid oxygen transfer characteristics in an aerobic submerged biofilter for the wastewater treatment. *Chemical Engineering Science* 47 (13):3745-3752.

Gillot, S., F. Kies, C. Amiel, M. Roustan, and A. Heduit. 2005. Application of the off-gas method to the measurement of oxygen transfer in biofilters. *Chemical Engineering Science* 60 (22):6336-6345.

Gunde, R., M. Dawes, S. Hartland, and M. Koch. 1992. Surface tension of wastewater samples measured by the drop volume method. *Environmental Science & Technology* 26 (5):1036-1040.

Hiatt, W. C., and C. P. L. Grady. 2008. An Updated Process Model for Carbon Oxidation, Nitrification, and Denitrification. *Water Environment Research* 80 (11):2145-2156.

Hidaka, T., and H. Tsuno. 2004. Development of a biological filtration model applied for advanced treatment of sewage. *Water Research* 38 (2):335-346.

Higbie, R. 1935. The rate of absorption of a pure gas into still liquid during short periods of exposure. *Trans. Am. Inst. Chem. Eng.* 31:365-389.

Kherbeche, A., J. Milnes, M. Jimenez, N. Dietrich, G. Hebrard, and B. Lekhlif. 2013. Multi-scale analysis of the influence of physicochemical parameters on the hydrodynamic and gas-liquid mass transfer in gas/liquid/solid reactors. *Chemical Engineering Science* 100:515-528.

Kies, F., S. Gillot, and A. Heduit. 2005. Paramètres influençant le transfert d'oxygène en biofiltres. In *10ème congrès de la SFGP : Récents progrès en génie des procédés*. Toulouse.

Lang, L., M. Pocquet, B. Ni, Z. Yuan, and M. Sperandio. 2016. Comparison of different 2-pathway models for describing the combined effect of DO and nitrite on the nitrous oxide production by ammonia-oxidizing bacteria. *Water Science & Technology*.

Leung, S. M., J. C. Little, T. Holst, and N. G. Love. 2006. Air/water oxygen transfer in a biological aerated filter. *Journal of Environmental Engineering-Asce* 132 (2):181-189.

Lizarralde, I., T. Fernandez-Arevalo, S. Beltran, E. Ayesa, and P. Grau. 2018. Validation of a multi-phase plant-wide model for the description of the aeration process in a WWTP. *Water Research* 129:305-318.

Maldonado, J. G. G., D. Bastoul, S. Baig, M. Roustan, and G. Hebrard. 2008. Effect of solid characteristics on hydrodynamic and mass transfer in a fixed bed reactor operating in co-current gas-liquid up flow. *Chemical Engineering and Processing* 47 (8):1190-1200.

Massara, T. M., S. Malamis, A. Guisasola, J. A. Baeza, C. Noutsopoulos, and E. Katsou. 2017. A review on nitrous oxide (N2O) emissions during biological nutrient removal from municipal wastewater and sludge reject water. *Science of the Total Environment* 596–597:106-123.

Mendoza-Espinosa, L., and T. Stephenson. 1999. *A Review of Biological Aerated Filters (BAFs) for Wastewater Treatment*. Vol. 16.

Ni, B. J., and Z. G. Yuan. 2015. Recent advances in mathematical modeling of nitrous oxides emissions from wastewater treatment processes. *Water Research* 87:336-346.

Pérez, J., J. L. Montesinos, and F. Gòdia. 2006. Gas–liquid mass transfer in an up-flow cocurrent packed-bed biofilm reactor. *Biochemical Engineering Journal* 31 (3):188-196.

Pocquet, M., Z. Wu, I. Queinnec, and M. Sperandio. 2016. A two pathway model for N2O emissions by ammonium oxidizing bacteria supported by the NO/N2O variation. *Water Research* 88:948-959.

Poughon, L., C. G. Dussap, and J. B. Gros. 1999. Dynamic model of a nitrifying fixed bed column: Simulation of the biomass distribution of Nitrosomonas and Nitrobacter and of transient behaviour of the column. *Bioprocess Engineering* 20 (3):209-221.

Reiber, S., and D. Stensel. 1985. Biologically Enhanced Oxygen Transfer in a Fixed-Film System. *Journal (Water Pollution Control Federation)* 57 (2):135-142.

Sander, R. 2015. Compilation of Henry's law constants (version 4.0) for water as solvent. *Atmospheric Chemistry and Physics* 15 (8):4399-4981.

Schreiber, F., P. Wunderlin, K. M. Udert, and G. F. Wells. 2012. Nitric oxide and nitrous oxide turnover in natural and engineered microbial communities: biological pathways, chemical reactions, and novel technologies. *Frontiers in Microbiology* 3.

Sperandio, M., and E. Paul. 1997. Determination of carbon dioxide evolution rate using on-line gas analysis during dynamic biodegradation experiments. *Biotechnology and Bioengineering* 53 (3):243-252.

Spérandio, M., M. Pocquet, L. Guo, B.-J. Ni, P. A. Vanrolleghem, and Z. Yuan. 2016. Evaluation of different nitrous oxide production models with four continuous long-term wastewater treatment process data series. *Bioprocess and Biosystems Engineering* 39 (3):493-510.

Sridhar, M. K. C., and C. Rami Reddy. 1984. Surface tension of polluted waters and treated wastewater. *Environmental Pollution Series B, Chemical and Physical* 7 (1):49-69.

Stenstrom, M. K., D. Rosso, H. Melcer, R. Appleton, V. Occiano, A. Langworthy, and P. Wong. 2008. Oxygen Transfer in a Full-Depth Biological Aerated Filter. *Water Environment Research* 80 (7):663-671.

Vaneeckhaute, C., F. H. A. Claeys, F. M. G. Tack, E. Meers, E. Belia, and P. A. Vanrolleghem. 2018. Development, implementation, and validation of a generic nutrient recovery model (NRM) library. *Environmental Modelling & Software* 99:170-209.

Vigne, E. 2007. Etude et modélisation dynamique d'un procédé par biofiltration en nitrification tertiaire. PhD thesis, Département de Génie Civil, Université Laval, Québec.

Vigne, E., J.-M. Choubert, J.-P. Canler, A. Héduit, K. Sorensen, and P. Lessard. 2010. A biofiltration model for tertiary nitrification of municipal wastewaters. *Water Research* 44 (15):4399-4410.

Viotti, P., B. Eramo, M. R. Boni, A. Carucci, M. Leccese, and S. Sbaffoni. 2002. Development and calibration of a mathematical model for the simulation of the biofiltration process. *Advances in Environmental Research* 7 (1):11-33.

Wang, Y., H. Fang, D. Zhou, H. Han, and J. Chen. 2016. Characterization of nitrous oxide and nitric oxide emissions from a full-scale biological aerated filter for secondary nitrification. *Chemical Engineering Journal* 299:304-313.

Tables

Table 1: Daily average operating conditions in the studied filtration unit (n = 14)

	NH_4^+ loading rate	NH_4^+ removal rate	Gas velocity	Liquid velocity	Dissolved N_2O	Emitted N_2O	Emitted / total N_2O*
	kgN/d		$m^3/m^2/d$		kgN/d		%
Mean	692	571	299	116	10.0	20.0	65
St. dev.	74	55	88	29	1.6	3.2	6

* Total N_2O corresponds to the sum of gaseous (= emitted) and liquid (= dissolved) fluxes as described in Bollon et al. (2016). It will be referred to as the N_2O production rate in this paper.

Table 2: Series of simulations performed and the associated gas-liquid transfer hypotheses

#	k_La_{O2}	ε_G	V_L =	Mass balance C_G	Remark
0	$17*U_G^{0.85}$	0.05	$V_R-V_M-V_B$	-	Base model
1	$43*U_G^{0.63}$	0.05	$V_R-V_M-V_B$	-	Using k_La to U_G curve from [a]
2	$43*U_G^{0.63}$	$f(U_G)^a$	$V_R-V_M-V_B$	-	Considering variable ε_G from [a] to calculate pressure
3	$43*U_G^{0.63}$	$f(U_G)^a$	$V_R-V_M-V_B-V_G$	-	Considering V_G to calculate V_L
4	$43*U_G^{0.63}$	$f(U_G)^a$	$V_R-V_M-V_B-V_G$	O_2	Considering gas O_2 depletion
5	$43*U_G^{0.63}$	$f(U_G)^a$	$V_R-V_M-V_B-V_G$	Complete	Considering gas N_2O and NO enrichment
6	$81*U_G^{0.63}$	$f(U_G)^a$	$V_R-V_M-V_B-V_G$	Complete	Final calibration of the transfer model

[a] Gillot et al. (2005)

Table 3: Summary of modeling results for each gas-liquid hypothesis.

#	NH_4^+ removal (%)	N_2O production rate (kgN/d)	N_2O-PF (% of N-NH_4^+ removed)	N_2O-EF (% of N-NH_4^+ removed)	Emitted / total (%)
Data	83	30.0	5.3	3.5	65
0	85	39.1	6.7	6.4	97
1	65	34.1	7.6	7.1	93
2	64	34.0	7.7	7.1	93
3	56	30.6	7.8	7.2	92
4	52	28.0	7.8	7.2	92
5	52	26.3	7.3	5.2	71
6	83	34.8	6.1	4.5	74

Figures

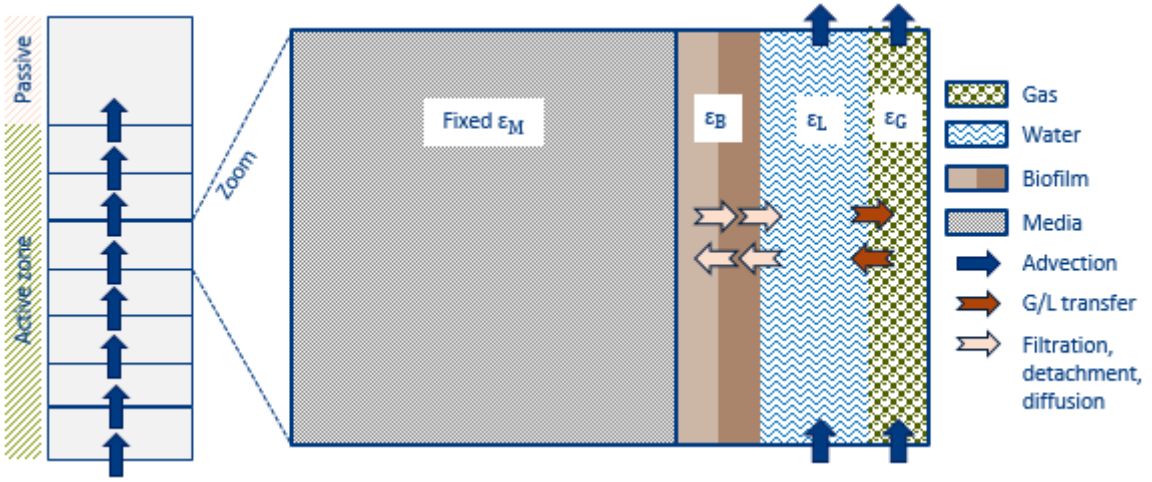

Figure 1: Schematic representation of the BAF model. Each compartment on the left side is a CSTR. ε_M is fixed (0.64), ε_G only depends on superficial gas velocity, ε_B varies with filtration, detachment and biomass growth, and ε_L is deduced from the other fractions.

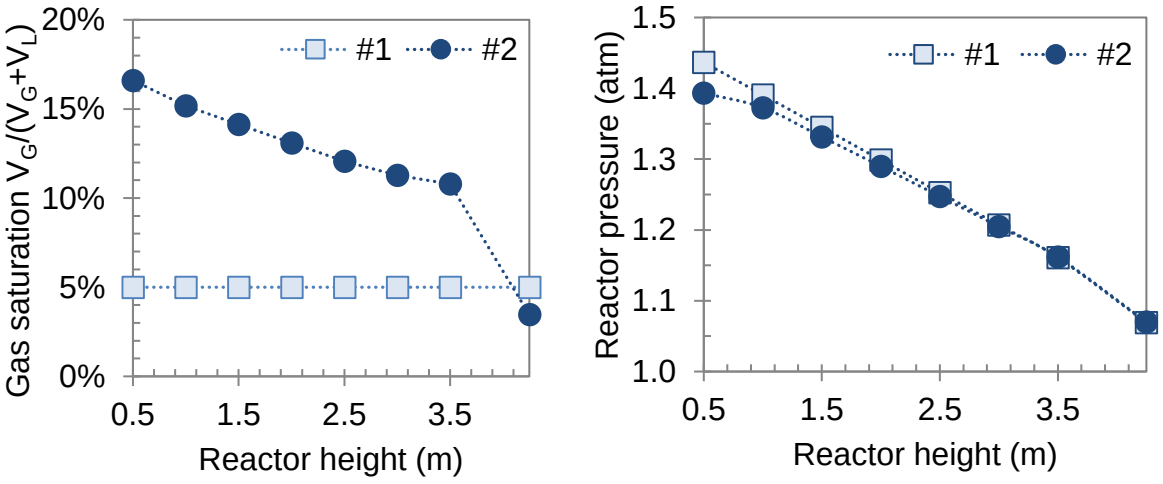

Figure 2: Evolution of air/liquid proportion (left) and pressure (right) over the BAF height before (#1) and after (#2) including a variable gas hold-up to calculate pressure.

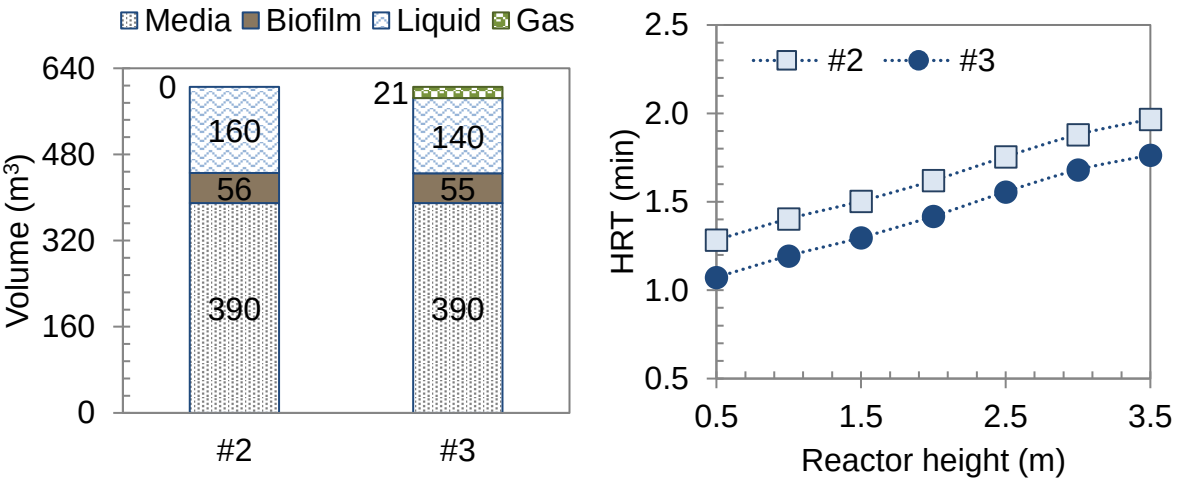

Figure 3: Prediction of compartment volumes in the active zone of the BAF (left) and evolution of HRT over the BAF height (right) before (#2) and after (#3) including gas hold-up to calculate V_L.

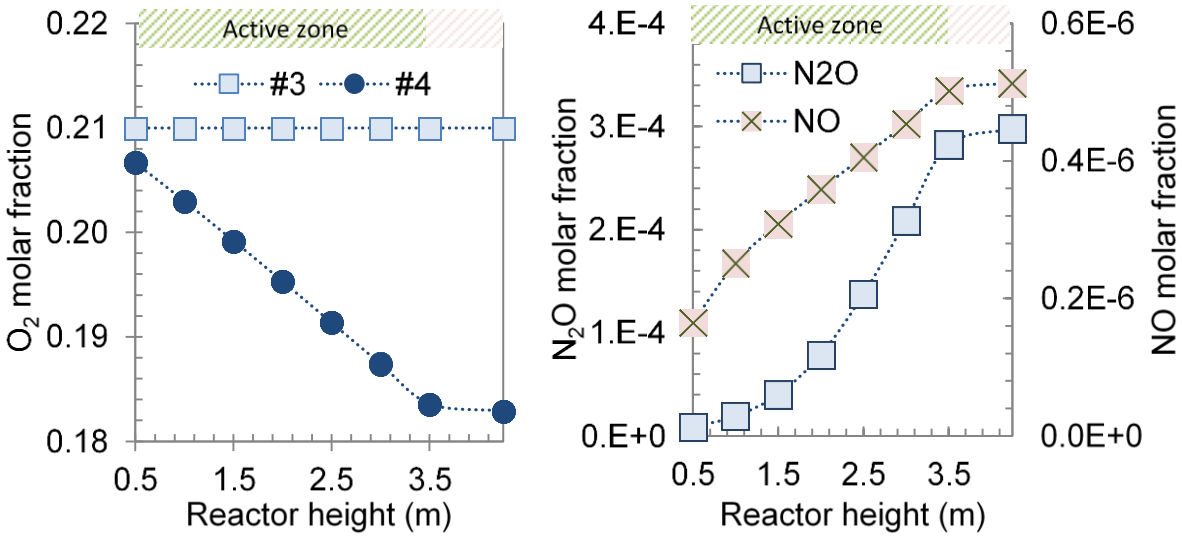

Figure 4: Gas molar fraction of O2 before (#3) and after (#4) including a mass balance (left); Gas molar fractions of NO and N2O after including a mass balance (right).

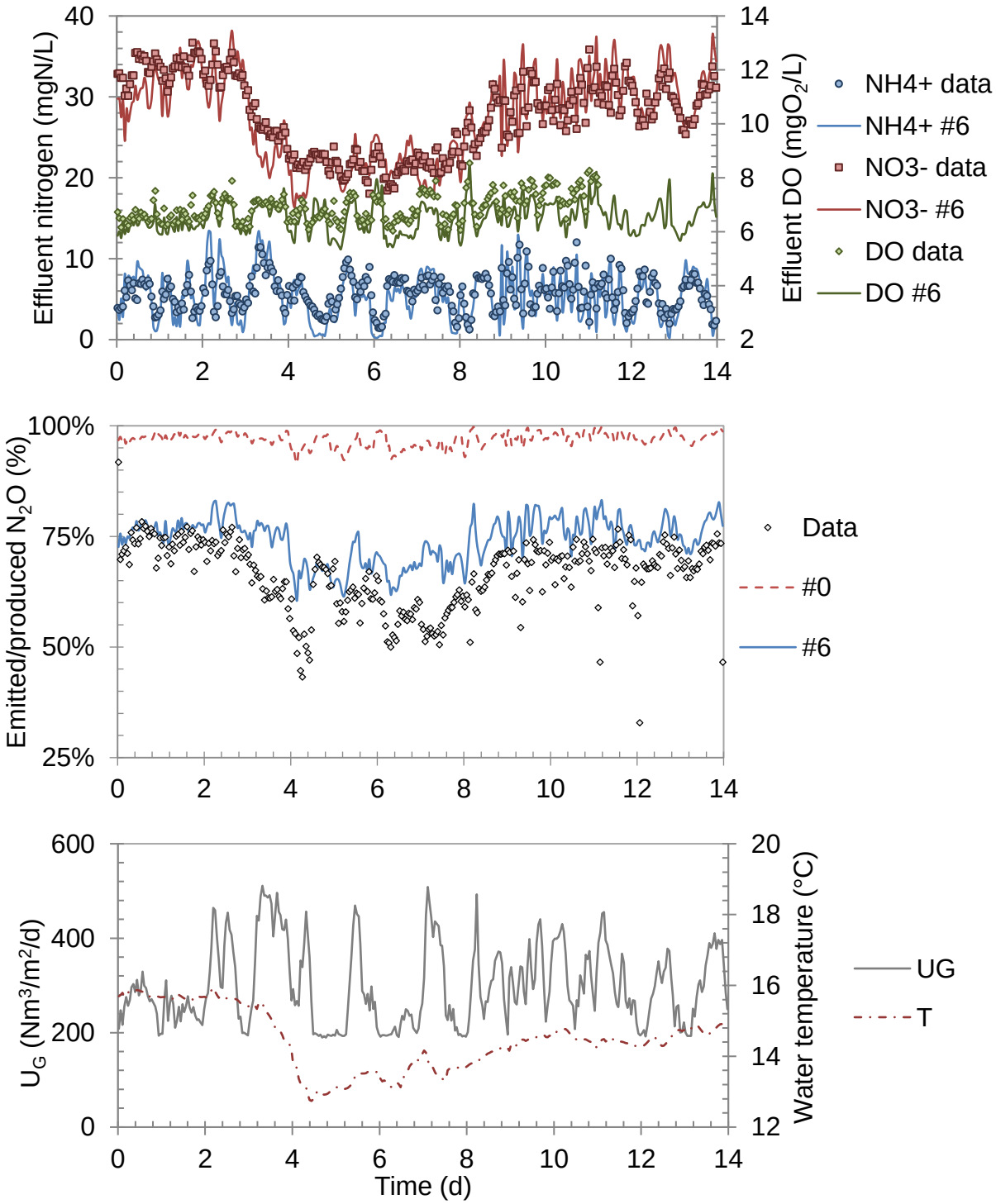

Figure 5: One-hour averaged predicted and measured effluent NH_4^+, NO_3^- and DO (top), emitted to produced N_2O predicted before (#0) and after (#6) including the mass balance on NO and N_2O (middle), superficial gas velocity and effluent temperature (bottom).